Customized Electronic Coupling in Self-Assembled Donor–Acceptor Nanostructures

By *Dimas G. de Oteyza,* Juan M. García-Lastra, Martina Corso, Bryan P. Doyle, Luca Floreano, Alberto Morgante, Yutaka Wakayama, Angel Rubio,* and *J. Enrique Ortega*

Charge transfer processes between donor–acceptor complexes and metallic electrodes are at the heart of novel organic optoelectronic devices such as solar cells. Here, a combined approach of surface-sensitive microscopy, synchrotron radiation spectroscopy, and state-of-the-art ab initio calculations is used to demonstrate the delicate balance that exists between intermolecular and molecule–substrate interactions, hybridization, and charge transfer in model donor–acceptor assemblies at metal-organic interfaces. It is shown that charge transfer and chemical properties of interfaces based on single component layers cannot be naively extrapolated to binary donor–acceptor assemblies. In particular, studying the self-assembly of supramolecular nanostructures on Cu(111), composed of fluorinated copper-phthalocyanines (F_{16}CuPc) and diindenoperylene (DIP), it is found that, in reference to the associated single component layers, the donor (DIP) decouples electronically from the metal surface, while the acceptor (F_{16}CuPc) suffers strong hybridization with the substrate.

1. Introduction

Nature itself is the most beautiful and irrefutable proof for the fascinating potential of supramolecular chemistry and self-assembly, which is exploited in creating sophisticated nano- and molecular machines capable of reliably carrying out varied and complex tasks. Meanwhile, scientists' attempts to artificially steer the self-assembly of designed nanodevices of comparable complexity and efficiency still collide with the greatly improving but still unsatisfactory understanding of supramolecular interactions and assembly processes on surfaces.[1] Enormous research efforts are thus currently devoted to further progress in our knowledge of the molecule–substrate and molecule–molecule interactions, which ultimately determine the crystalline and electronic structure, and consequently the functionality of the self-assembled system.[2] One of the possible routes to improve this knowledge is to address the molecule–substrate interactions in systems with systematically varied intermolecular interactions, and vice versa.[3–8] In particular, the use of molecular mixtures allows tuning of the intermolecular interactions by a convenient choice of molecules with complementary functional groups. By these means, comparison of single component and binary layers can provide systems with distinctly different intermolecular interactions, in which to study their effect on the interrelated molecule–substrate interactions.[4–8] In addition, research on donor–acceptor nanostructured mixtures undoubtedly possesses an inherent relevance for optoelectronic devices such as photovoltaic cells.[9] Studies on binary supramolecular assemblies therefore do not only bear enormous interest from a fundamental point of view, but also in direct relation to applications if molecules with appropriate semiconducting properties are combined.

Simultaneous characterization of the interdependent structural and electronic properties is required for a thorough understanding of the systems under study. However, while numerous studies over the last years have been focused on structural properties of multicomponent organic films,[9,10] scarce research efforts have been devoted to their electronic structure.[4–8] With this aim, we have made use of a number of complementary experimental techniques to study self-assembled layers on Cu(111) single crystals of

[*] Dr. D. G. de Oteyza, Dr. M. Corso, Prof. J. E. Ortega
Donostia International Physics Center
Paseo Manuel Lardizabal 4, 20018 San Sebastián (Spain)
E-mail: d_g_oteyza@ehu.es
Dr. D. G. de Oteyza, Dr. Y. Wakayama
Advanced Electronic Materials Center
National Institute for Materials Science
1-1 Namiki, Tsukuba 305-0044 (Japan)
Dr. J. M. García-Lastra, Prof. A. Rubio
Nano-Bio Spectroscopy group and European Theoretical Spectroscopy Facility (ETSF)
Departamento Fisica de Materiales UPV/EHU
Apdo. 1072, San Sebastián (Spain)
Dr. B. P. Doyle, Dr. L. Floreano, Prof. A. Morgante
Laboratorio Nazionale TASC
INFM-CNR National
Area Science Park, I-34012 Basovizza, Trieste (Italy)
Prof. J. E. Ortega
Centro de Fisica de Materiales
Materials Physics Center, CSIC-UPV/EHU
Paseo Manuel Lardizabal 3, 20018 San Sebastián (Spain)
and
Departamento de Fisica Aplicada, UPV/EHU
Plaza de Oñate 2, 20018 San Sebastián (Spain)

DOI: 10.1002/adfm.200901374

diindenoperylene (DIP) and fluorinated copper-phthalocyanines (F_{16}CuPc), two molecules typically used as donor and acceptor semiconductors, respectively, in organic devices.[11] Their geometrical arrangement are investigated by scanning tunneling microscopy (STM). For the electronic properties, core-level (XPS) and valence band (UPS) photoelectron spectroscopy are used. XPS provides chemical information on the system and therefore allows the detection of, for example, charge-transfer effects. In addition, it also gives insight into changes of other electronic properties such as core-hole screening by the substrate, which in turn reflects changes in the molecule–substrate electronic coupling. UPS allows the determination of the electron injection barrier from the organic overlayer into the metallic substrate and also holds information about potential molecule–substrate hybridization via the impact of the overlayer on the substrate valence band. While XPS and UPS deal with occupied electronic levels, the unoccupied orbitals are probed by near edge X-ray absorption fine structure spectroscopy (NEXAFS). Lastly, we have performed density functional theory (DFT) calculations to corroborate and understand our experimental findings on the crystalline and electronic structure, as well as to get quantitative information on relevant issues such as the strength of the interactions responsible for the self-assembly. By combining the results of the various experimental techniques and theoretical calculations, each of which by itself provides only limited information, we finally arrive at a fully coherent picture of the dependence of the molecule–substrate electronic coupling on their specific supramolecular environment.

2. Results and Discussion

Upon F_{16}CuPc deposition onto Cu(111), the molecules at the interface adopt a lying down configuration and form an ordered monolayer, as depicted in Figure 1a.[12] The corresponding lattice is described by an oblique unit cell with parameters $a = 14.5 \pm 0.5$ Å, $b = 14.5 \pm 0.5$ Å, and $\gamma = 75 \pm 2^\circ$ and thus, within the error margins, comparable with the geometry observed on Au(111).[5] The a-axis is aligned along the [−110] and equivalent directions. Along these directions we find long-range order. However, perpendicular to it, we find the presence of two glide domains (half cell translation plus mirror domain with a common a-axis, as shown in Figure 1a) and frequent domain boundaries among them.[12] In the case of DIP, the monolayer on Cu(111) displays two different molecular arrangements depending on the width of the terrace on which it assembles. On wider terraces only a short range ordered phase is formed, while confinement effects trigger the formation of a long range ordered phase on narrower terraces with widths of 15 nm downward.[13] Given the coexistence of molecular arrangements, the similar azimuthal molecular orientation (pointing to comparable molecule–substrate interactions), and the advantages of periodic structures for later theoretical analysis, we will from now on focus on the long range ordered phase, described by an oblique unit cell of parameters $a = 8.7 \pm 0.4$ Å, $b = 18.5 \pm 0.7$ Å, and $\gamma = 71 \pm 1^\circ$ (Fig. 1b).[13]

As compared to the single component layers, in which the absence of complementary functional groups or dipolar moments limits the intermolecular interactions to weak van der Waals interactions and steric effects, the combination of fluorine surrounded F_{16}CuPc and hydrogen surrounded DIP molecules in binary layers greatly enhances the intermolecular interactions via C−H···F−C bonds.[5,14] As a consequence, the molecules mix into an ordered phase as shown in Figure 1c, in which each molecule is surrounded by molecules of the other species to maximize the C−H···F−C interactions.[14] The primitive unit cell presents the following parameters $a = 21.3 \pm 1$ Å, $b = 19.4 \pm 1$ Å, and $\gamma = 123 \pm 2^\circ$, and comprises one F_{16}CuPc and one DIP molecule. Interestingly, the higher contrast of F_{16}CuPc in the STM images as compared to DIP, corresponding to an apparent height difference of ∼0.4 Å (Fig. 1c), is observed independently of the measurement conditions (current, voltage, and polarization). It is therefore interpreted as a topographic signature, rather than an electronic effect, which would present dependence on the bias.

Previous studies have shown the molecule–substrate distances to vary as a result of modified intermolecular interactions.[3–5] Now the question arises, whether the observed height difference among both molecules in the binary layers is a result of the new interactions in the mixed layers or just similar to that between the molecules in single component layers. In order to get an answer, we have determined the optimized packing structure of the different molecular monolayers by means of first principles calculations using DFT. The results are shown in the lower panels of Figure 1, depicting a top-view of the respective molecular arrangements. As observed from the different atom-substrate distances, which are summarized in Table 1, molecular distortions deviating from a planar molecular arrangement become evident, which are in good agreement with previous X-ray standing-wave measurements of F_{16}CuPc on Cu(111).[15] Calculations show that the atom–substrate distances of both molecular species upon molecular mixture follow a similar trend: the distorted molecular shape is maintained, and the molecule–substrate distance is slightly increased by ∼0.06 Å. In spite of the fact that intermolecular interactions would be optimized by a coplanar molecular arrangement, molecule–substrate

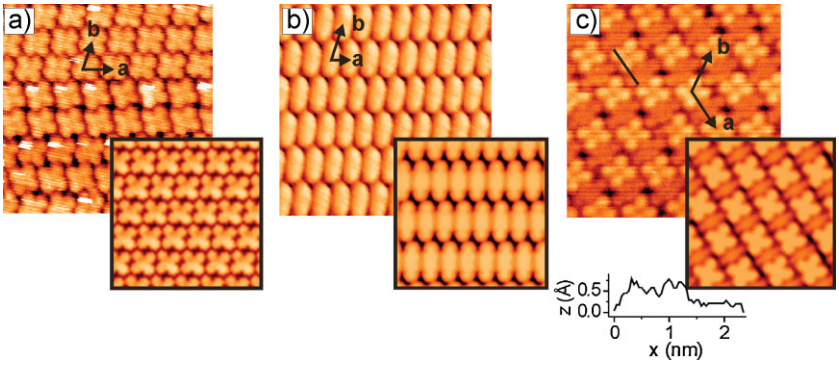

Figure 1. Constant current STM images (10 nm × 10 nm) taken on single-component a) F_{16}CuPc and b) DIP layers, as well as on c) binary layers. The unit cell vectors are overlaid on the image. The simulated STM images resulting from the optimized packing geometry are depicted under the experimental data. In the case of the binary layer, a "topographic" profile along the black line in the STM image is shown to highlight the "height" difference between F_{16}CuPc and DIP.

Table 1. Average atom-substrate distances (in Å) for the different atomic species in $F_{16}CuPc$ and DIP in single-component and binary layers.

	DIP	$F_{16}CuPc$		Mixed layer
		DFT	Experimental [a]	
C (DIP)	2.18	–	–	2.26
H (DIP)	2.37	–	–	2.41
C ($F_{16}CuPc$)	–	2.57	2.61	2.63
N ($F_{16}CuPc$)	–	2.54	2.70	2.58
F ($F_{16}CuPc$)	–	2.69	2.88	2.75
Cu ($F_{16}CuPc$)	–	2.39	–	2.46

[a] Values taken from Ref. [15].

interactions dominate and determine the distance to the substrate, which is ~0.4 Å higher for the $F_{16}CuPc$ than for DIP (taking C atoms as a reference), being consistent with the topographic origin of the observed contrast in the STM images. Simulated STM images based on the theoretically optimized adsorption structures are shown in Figure 1. The reliability of the calculations is thus proven by the excellent agreement with the experimental findings both in the lateral arrangement and in the molecule–substrate distances.

The calculations provide us with further insight into the relevant interactions in the self-assembled phases. In particular, the adsorption energy of $F_{16}CuPc$ and DIP in the single component layers is 7.82 and 7.78 eV, respectively. These high values imply a strong molecule–substrate interaction. In fact, according to Mulliken population analysis, a significant charge transfer to the Cu substrate takes place from both molecular species (0.367 e for DIP and 0.528 e for $F_{16}CuPc$). [16] A plot of the projected density of states on the highest occupied molecular orbital (HOMO) and lowest unoccupied molecular orbital (LUMO) of DIP and $F_{16}CuPc$ for the single component and the mixed layers is shown in Figure 2a. Both molecules have their HOMO levels close to the Fermi edge. As a consequence, their high-energy tails exceed the Fermi energy and therewith enable charge transfer to the substrate. A map of the electron density redistribution upon molecular adsorption is depicted in Figure 2b.

Such strong electronic coupling between molecules and substrate is additionally confirmed experimentally by our NEXAFS measurements. Figure 3 shows the C K-edge spectra measured on the different molecular monolayers under p- and s-polarizations.[17] The peaks account for the resonances of core electron excitations into π^* or σ^* molecular orbitals, and the steps for excitations to a continuum or quasi-continuum of final states.[17] Interestingly, we find the presence of two well defined steps. Masked by the strong intensity of the π^* resonances at p-polarization due to the lying down molecular configuration,[17] the steps are best discerned under s-polarization. The most common step observed in NEXAFS spectra of molecules adsorbed on surfaces occurs at the ionization threshold, that is, upon excitation of the core electrons to the vacuum level (VL). An additional step may occur due to excitations into the densely spaced electronic states of the metal above the Fermi level (FL), if a strong electronic coupling of molecule and substrate is present. In such a case, the FL step should be located at the core level binding energy,

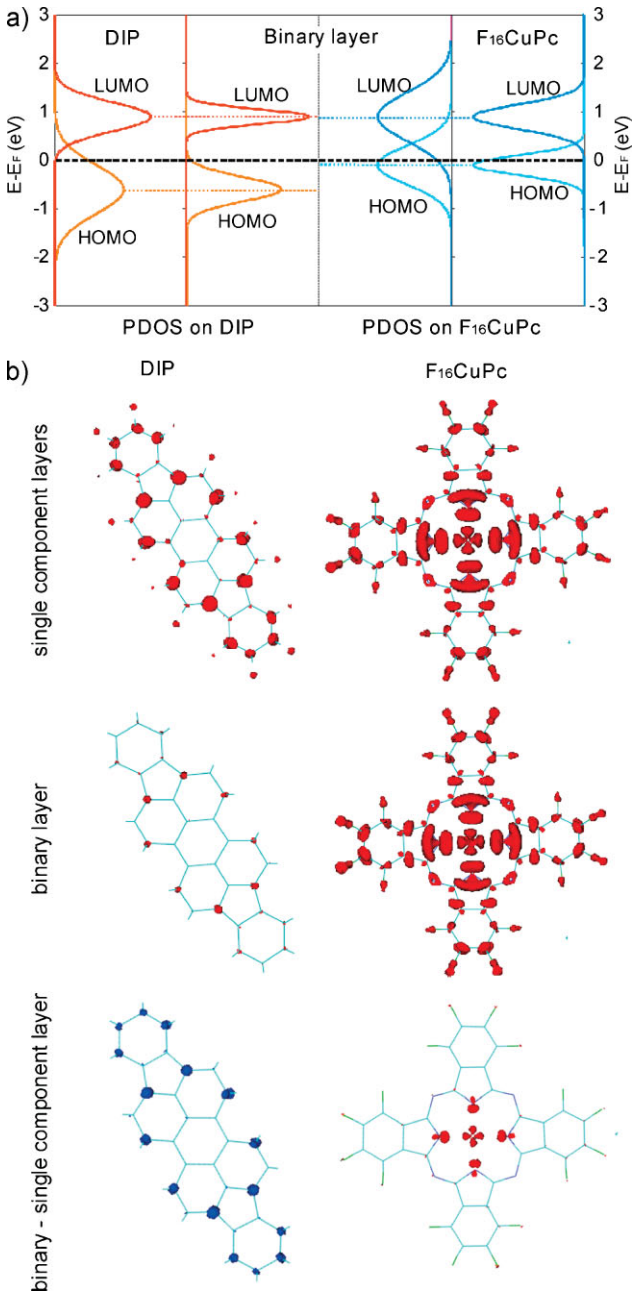

Figure 2. a) Projected density of states on the HOMO and LUMO of $F_{16}CuPc$ and DIP for the single component and binary layers. b) Difference in the electronic densities with respect to the isolated molecules for $F_{16}CuPc$ and DIP in the single-component and binary layers. For comparison purposes, the difference in the electronic densities between the single and mixed layers is also represented. The represented isosurfaces in red (blue) contain the points where the electronic density lessens (increases) by 0.0008 e^-.

and the difference in energy between both steps represents the work function.[17] The observed steps present a qualitative agreement with these requirements. The FL step is located around ~286 eV and thus in reasonable proximity, as will be shown later, to the core-level binding energies. Even better agreement is observed in the

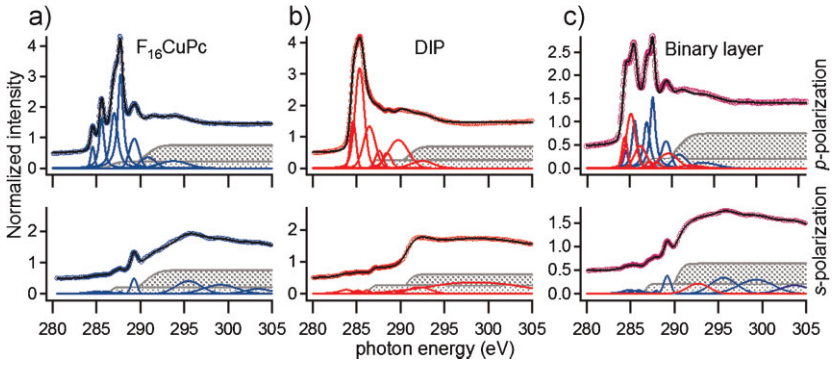

Figure 3. C K-edge NEXAFS spectra (symbols) of the single-component a) F_{16}CuPc and b) DIP layers, as well as c) that of the binary layer, under s- (bottom) and p-polarizations (top). The spectra have been fitted (solid line) with a number of peak and step functions represented under the corresponding spectra.

estimated work function of about ~4 eV, given the VL step position around ~290 eV. Clean Cu(111) has a work function of 4.95 eV.[18] However, the work function is typically lowered by the formation of an interface dipole upon molecular adsorption. Taking as a reference the dipole formed for monolayers of another conjugated molecule on Cu(111) such as benzene, which lowers the work function by 1 eV,[19] we arrive at the observed work function value of ~4 eV. All the above, together with the weakening of the FL step in NEXAFS spectra measured on thick films, prove its origin from excitations of molecules at the interface into metal empty states, and therewith confirm the strong electronic coupling predicted by the calculations.[20]

Upon molecular mixture and according to the theoretical charge transfer analysis, we find charge transfer into the substrate of 0.140 e for DIP and 0.594 e for F_{16}CuPc molecules in the binary layers.[16] Thus, as compared to the single component layers, the transfer from F_{16}CuPc remains roughly the same, while that of DIP is considerably reduced. As depicted in Figure 2a, the position of the corresponding HOMO and LUMO orbitals upon molecular mixture remain unchanged. However, their width is dramatically modified, being approximately doubled (halved) as a result of an enhanced (reduced) hybridization of F_{16}CuPc (DIP) with the substrate in the binary layer. Because the F_{16}CuPc HOMO is centered close to the FL, a change in its width hardly affects the charge transfer, while for DIP it is noticeably reduced upon the narrowing of its deeper lying HOMO level. The changes in electron density upon molecular adsorption in the binary layer as compared to the free standing molecules are depicted in Figure 2b. In addition, the difference in electron density between the molecules in single component and in binary layers is shown in the lower panel. These plots show in a graphic way how the charge transfer from DIP to the substrate is strongly reduced in the binary layer (leading to a final electron density distribution very close to that of the isolated molecule), while the opposite trend (though to a lower extent) is obtained for F_{16}CuPc. We also find from the calculations that the energy gained by the intermolecular C−H···F−C interactions is 1.16 eV per F_{16}CuPc-DIP pair. Interestingly, the adsorption energy per F_{16}CuPc-DIP pair is 17.28 eV, and thus 1.68 eV higher than the sum of the F_{16}CuPc and DIP adsorption energies in single-component layers. This increase may have its origin in substrate-mediated intermolecular interactions, and/or modified molecule–substrate interactions in the binary layers. Proof for the latter is given by the dramatically modified hybridization of the molecules with the substrate observed in Figure 2a. Most interestingly, hybridization is enhanced for F_{16}CuPc in the binary layer. The opposite trend was observed in the case of F_{16}CuPc and DIP binary layers on Au(111),[5] a substrate generally leading to weaker molecule–substrate interactions. This evidences the crucial role of the substrate and the delicate correlations between intermolecular and molecule–substrate interactions. An increased hybridization in supramolecular assemblies with enhanced intermolecular interactions as observed on Cu(111) seems counterintuitive,[4,5] but has nevertheless been similarly observed for other donor–acceptor assemblies presenting strong molecule–substrate interactions.[7]

An experimental confirmation of the hybridization of the molecular orbitals is given by the valence band photoelectron spectra in Figure 4. For the clean substrate, the main features appear between ~2 and ~5 eV and correspond to the Cu 3d levels.[21,22] Upon DIP adsorption, the spectrum shows only minor changes. The same applies for F_{16}CuPc adsorption, where the main changes correspond to the new features appearing at 10.30 and 11.68 eV associated with the fluorine 2p levels. However, upon adsorption of the binary layer, the features corresponding to the Cu 3d levels are dramatically modified and evidence strong hybridization with the organic overlayer. The dominating −3.55 peak exhibits a clear split-off shoulder at −4.30 eV, which can be readily assigned to substrate Cu atoms in close contact with the organic overlayer. In fact, symmetry arguments for the Cu 3d orbitals indicate that the −3.55 eV is the most sensitive to adsorbate re-hybridization. [21–23]

We have made use of combined photoemission and absorption spectroscopy measurements to discriminate the molecular species where major re-hybridization takes place. Figure 5 shows the low-energy region of the C K-edge NEXAFS spectrum measured on the binary layer. Given the 1 to 1 molecular ratio in the binary layer, and the same number of C atoms in each molecule, the spectrum is

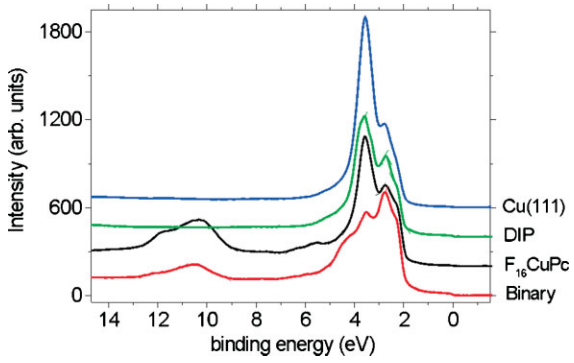

Figure 4. Valence-band photoelectron spectra taken with an excitation energy of 130 eV on the clean Cu(111) substrate, the single-component F_{16}CuPc and DIP layers, and on the binary layer.

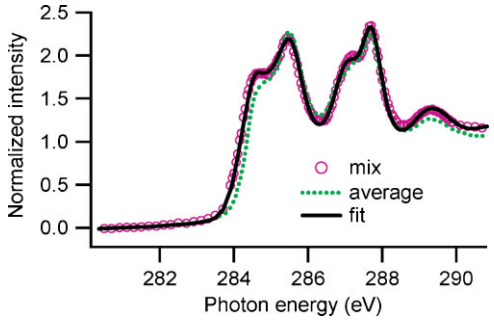

Figure 5. Experimental C K-edge spectrum of the binary layer (symbols), together with the arithmetic mean of the F_{16}CuPc and DIP spectra (dotted green line), and a fit to the data (solid black line). In the fit, the peaks of the fitted DIP spectrum, previously shifted rigidly by 0.2 eV, have been summed to the peaks of the fitted F_{16}CuPc spectrum. Then, only the intensities have been subject to minor adjustments.

expected to equal the arithmetic mean of F_{16}CuPc and DIP spectra. However, a clear shift of 0.2 eV is evident in the low-energy onset. In this energy region, contributions of both DIP and F_{16}CuPc mix together (Fig. 3), while the features observed around 288 eV correspond mainly to F_{16}CuPc contributions (Fig. 3). When comparing the measured spectrum and the averaged one no shift is observed in these latter features, so we conclude that the shift in the onset region corresponds to changes in the DIP electronic levels. In fact, applying a rigid shift of 0.2 eV to all resonances resulting from the fit to the DIP C K-edge spectrum (Fig. 3), summed with the resonances of the F_{16}CuPc spectrum (Fig. 3), and with minor changes solely to the peak intensities, provides an excellent fit to the experimental data (Fig. 5).[24,25] The naive interpretation as a lowering of the unoccupied DIP energy levels would disagree with the theoretical calculations, which predict an unchanged DIP LUMO alignment. However, final and initial state effects mix together in NEXAFS spectra. Additional core-level photoemission measurements shown below provide us with the understanding of the shift of the DIP levels.

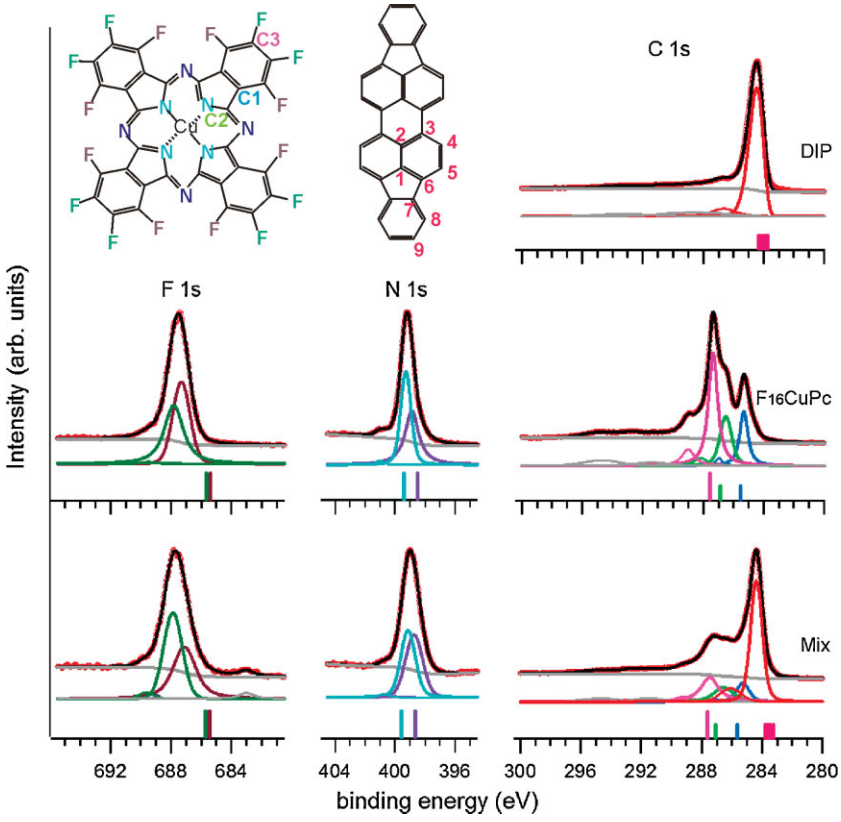

Figure 6. F 1s, N 1s, and C 1s core-level photoelectron spectra measured on single-component DIP and F_{16}CuPc molecular monolayers, as well as on mixed binary monolayers. The experimental data are depicted by red symbols and the corresponding fits by the overlaid black solid lines. The individual fitting components (background and peaks) are shown below. The correspondence between the main peaks and the specific atoms is given by the colors of lines and atom labels in the schematic molecular representations. First order shake-up satellites (arising from simultaneous HOMO–LUMO transitions) are colored as the corresponding main peaks. Higher order shake-up satellites (observed up to ~10 eV larger binding energies than the main peaks in the C spectra) are colored gray. In the case of DIP, the core levels of the nine chemically different atoms are very close in energy. As an approximation, the spectrum is fitted by an asymmetric single peak and a single shake-up satellite. At the bottom of the graphs, colored bars mark the positions of core levels according to DFT calculations (shifted all together by 2.8 eV to lower binding energies to better fit the experimental data).

Core-level photoelectron spectra of the various atomic species in single component and binary molecular layers are summarized in Figure 6, together with the calculated binding energies for each one of the components.[26] Interestingly, the C 1s line in DIP is at lower binding energy than the manifold F_{16}CuPc peaks, thereby allowing us to discriminate between the different contributions and analyze molecule dependent changes upon mixing. Comparison of the spectra of single-component and binary layers shows significant alterations. First of all, the width of the C 1s peak of DIP decreases in the mixed layer by ~20%, accompanied by a shift to lower binding energy by 0.14 eV. Both the reduced width and the shift may be simply explained by a decreased electronic coupling between molecule and substrate, and lower charge transfer from molecule to substrate in the mixed layer. The magnitude and direction of the shift in the C 1s DIP peak are consistent with the shift in the NEXAFS spectrum and prove its origin in initial state effects due to the reduced charge transfer of DIP in the mixed layers.

The peaks corresponding to F_{16}CuPc all show considerably increased widths (ranging from 30 to 70% depending on the peak). The peak positions show different trends, remaining virtually unchanged for C, with minor shifts to lower binding energy (close to the resolution limits) for F, and shifted toward lower binding energy by 0.14 eV for N. As opposed to the case of DIP, the large increase in the F_{16}CuPc core-level widths implies strong metallization, that is, hybridization with the substrate.[4–7] In the absence of significant charge-transfer changes, a stronger hybridization provides a more effective screening of the core holes and

therefore lowers their binding energy.[6] Because the molecular orbitals closest in energy to the Fermi edge (both HOMO and LUMO) are mainly located on the central Cu and N atoms, the enhanced screening affects more strongly the N core levels than those of C and F.[5]

3. Conclusions

By combining all our results from different experimental techniques and theoretical calculations, we finally arrive at a fully coherent and comprehensive picture of the self-assembly of donor–acceptor nanostructures, their crystalline structure, and electronic properties. Most importantly, we find essential differences in the electronic coupling between molecules and substrate comparing single component and binary layers, shedding new light on the complex correlations between intermolecular and molecule–substrate interactions. While DIP is decoupled electronically from the substrate in the mixed layer with enhanced intermolecular interactions, F_{16}CuPc suffers major hybridization with the substrate. Most studies on interfacial electronic properties, which are key factors for charge carrier injection/extraction and thus for the functionality of organic based optoelectronic devices, have been performed on model single-component molecular layers on metals. Nanostructured donor–acceptor systems are expected to play a key role in future development of organic devices, but have been mostly studied from a structural and only scarcely from an electronic point of view. We show that the properties of single-component layers cannot be naively extrapolated to the new molecular environments of supramolecular assemblies. This makes it an ineluctable requirement to address the electronic properties of multi-component systems, if a thorough understanding of their interrelation with structural aspects, which would eventually allow a rational design of functional donor–acceptor nanostructures with optimized properties, is to be obtained.

4. Experimental

The Cu(111) surface was prepared by repeated Ar^+ sputtering and annealing cycles. The molecules were purified twice by gradient sublimation before use, and were evaporated from a Knudsen cell with deposition rates between 0.05 and 0.1 monolayer (ML) per minute. The binary layers were prepared by simultaneous molecular co-deposition at substrate room temperature.

The STM measurements were performed at room temperature in constant current mode with chemically etched tungsten tips in a commercial JEOL UHV system including two interconnected growth and measurement chambers, each with base pressures in the 10^{-10} mbar range. The substrate surface was checked prior to film growth, requiring the observation of clean and large terraces. The image processing and data analysis were performed with the WSxM software [27].

The core-level and valence-band photoelectron spectroscopy, as well as the NEXAFS measurements, were performed at the beamline ALOISA of the synchrotron light source ELETTRA in Trieste (Italy). Prior to evaporation, the surface was checked for its cleanliness and order by XPS and reflection high energy electron diffraction (RHEED). The sample coverage was monitored by means of a quartz crystal microbalance, assuming a density of 2 g cm^{-3} for F_{16}CuPc and 1.3 g cm^{-3} for DIP [28], and further crosschecked with an analysis of the Au 4f and C 1s core level intensities. The manipulator is coaxial with the photon beam, which allows changing the orientation of the surface with respect to linear polarization of the beam while keeping constant the grazing angle (set to 4° in these experiments), i.e., without changing the beam footprint on the sample. For more details about the scattering geometry, see Ref. [29]. NEXAFS spectra were taken in partial electron yield. Spectra measured at the C K-edges were calibrated by acquisition of the 1s–π^* gas phase transitions of CO at $h\upsilon = 287.4$ eV [30]. The photoemission data shown in Figures 5 and 6 were taken with excitation energies of 130 eV for the valence band, 500 eV for the C and N core levels, and 800 eV for the F core level, with pass energies of 10, 20, and 30 eV, respectively. The spectrometer resolution is 1% of the pass energy.

Two kinds of calculations have been carried out in this work, both in the framework of DFT. Firstly, we have studied the photoemission spectra from the core levels of the different ions of both molecules, DIP and F_{16}CuPc, by means of the Amsterdam Density Functional (ADF) package [31], using the ΔSCF methodology. The local density approximation (LDA) exchange-correlation energy was computed using the Vosko-Wilk-Nussair (VWN) functional [32]. All the atoms have been described through basis sets of TZP quality (triple-ζ Slater-type orbitals plus one polarization function) given in the program database. Obviously, since the core electrons have to be removed from the molecule in order to get the photoemission energy, these calculations are all-electron. Due to the technical difficulties of the ΔSCF methodology for core electrons, we have studied the isolated molecules in vacuo, optimizing their respective geometries in their ground states.

Secondly, the calculations of the geometries of the DIP and F_{16}CuPc single-component and binary layers on the Cu(111) surface were performed with the SIESTA code [33]. The charge transfer between molecules and substrate (obtained by means of the Mulliken analysis), the densities of states (DOS), and the simulated STM images were also obtained from these calculations. The LDA exchange-correlation energy was computed using the Perdew-Wang (PW) functional [34]. The use of different LDA functionals in ADF and Siesta calculations is not relevant for the results presented in this work. All the atoms have been described through basis sets of DZP quality (double-ζ Slater-type orbitals plus one polarization function) and the core electrons were represented through the Fritz-Haber Institute (FHI) library's pseudopotentials for PW functional (1s for C, N, F, and 1s–3p for Cu) [35]. Because the molecules are strongly chemisorbed on the surface, it is not expected that the presented results change substantially by including the effect of Van der Waals forces in the calculations, as recently reported for benzene on Cu(110) [36]. Due to the size of the systems, only the Γ point has been taken into account. Only a double Cu layer is used to model the substrate, since in the case of the binary layer it is not feasible to go beyond. This approach has been previously justified checking the convergence of the results with single component layers of DIP and F_{16}CuPc and 4, 3, and 2 layers of Cu as substrate. In order to keep the calculations affordable, we have forced commensuration between the organic overlayer lattice and the Cu(111) substrate (always within the experimental errors from STM). In all the calculations the lattice parameters were kept fixed and only the internal coordinates of the molecules were allowed to vary.

Acknowledgements

We thank J. Pflaum and S. Hirschmann for purification of the molecules, and A. Cossaro and A. Verdini for support during our measurements in ELETTRA. This work was supported by the European Community through the Integrated Infrastructure Initiative ''European Light Sources Activities – Synchrotrons and Free Electron Lasers''. The work was further supported through the Spanish Ministerio de Educación y Ciencia (MAT2007-63083, FIS2007-65702-C02-01), ''Grupos Consolidados UPV/EHU del Gobierno Vasco'' (IT-319-07, IT-257-07), CSIC, and the European Community throughe-I3 ETSF project (Contract Number 211956), and NANO-ERA CHEMISTRY. We acknowledge support by the ''Red Espanola de

Supercomputacion'' and SGIker ARINA(UPV/EHU). J. M. G.-L. acknowledges funding Spanish MEC through Juan de la Cierva program.

Received: July 23, 2009
Published online: October 8, 2009

[1] a) J.-M. Lehn, *Science* **2002**, *295*, 2400. b) D. N. Reinhoudt, M. Crego-Calama, *Science* **2002**, *295*, 2403.

[2] a) J. V. Barth, G. Costantini, K. Kern, *Nature* **2005**, *437*, 671. b) J. V. Barth, *Annu. Rev. Phys. Chem.* **2007**, *58*, 375.

[3] a) C. Stadler, S. Hansen, I. Kröger, C. Kumpf, E. Umbach, *Nat. Phys.* **2009**, *5*, 153. b) L. Kilian, A. Haushild, R. Temirov, S. Soubatch, A. Schöll, A. Bendounan, F. Reinert, T.-L. Lee, F. S. Tautz, M. Sokolowski, E. Umbach, *Phys. Rev. Lett.* **2008**, *100*, 136103-1-4.

[4] K. J. Franke, G. Schulze, N. Henningsen, I. Fernandez-Torrente, J. I. Pascual, S. Zarwell, K. Rück-Braun, M. Cobian, N. Lorente, *Phys. Rev. Lett.* **2008**, *100*, 036807-1-4.

[5] D. G. de Oteyza, I. Silanes, M. Ruiz-Oses, E. Barrena, B. P. Doyle, A. Arnau, H. Dosch, Y. Wakayama, J. E. Ortega, *Adv. Funct. Mater.* **2009**, *19*, 259.

[6] I. Fernandez-Torrente, K. J. Franke, J. I. Pascual, *J. Phys. Cond. Matter* **2008**, *20*, 184001-1-11.

[7] N. Gonzalez-Lakunza, I. Fernandez-Torrente, K. J. Franke, N. Lorente, A. Arnau, J. I. Pascual, *Phys. Rev. Lett.* **2008**, *100*, 156805-1-4.

[8] M. Ruiz-Oses, D. G. de Oteyza, I. Fernandez-Torrente, N. Gonzalez-Lakunza, P. M. Schmidt-Weber, T. Kampen, K. Horn, A. Gourdon, A. Arnau, J. E. Ortega, *ChemPhysChem.* **2009**, *10*, 896.

[9] R. Otero, D. Ecija, G. Fernández, J. M. Gallego, L. Sanchez, N. Martín, R. Miranda, *Nano Lett.* **2007**, *7*, 2602.

[10] a) M. de Wild, S. Berner, H. Suzuki, H. Yanagi, D. Schlettwein, S. Ivan, A. Baratoff, H.-J. Guentherodt, T. A. Jung, *Chem. Phys. Chem.* **2002**, *10*, 881. b) S. Yoshimoto, Y. Honda, O. Ito, K. Itaya, *J. Am. Chem. Soc.* **2008**, *130*, 1085. c) M. Treier, M.-T. Nguyen, N. V. Richardson, C. Pignedoli, D. Passerone, R. Fasel, *Nano Lett.* **2009**, *9*, 126. d) J. A. Theobald, N. S. Oxtoby, M. A. Phillips, N. R. Champness, P. H. Beton, *Nature* **2003**, *424*, 1029. e) L. Scudiero, K. W. Hipps, D. E. Barlow, *J. Phys. Chem. B* **2003**, *107*, 2903. f) W. Chen, H. Li, H. Huang, Y. Fu, H. L. Zhang, J. Ma, A. T. S. Wee, *J. Am. Chem. Soc.* **2008**, *130*, 12285. g) M. E. Cañas-Ventura, W. Xiao, D. Wasserfallen, K. Müllen, H. Brune, J. V. Barth, R. Fasel, *Angew. Chem, Int. Ed.* **2007**, *46*, 1814.

[11] a) N. Karl, K.-H. Kraft, J. Marktanner, M. Münch, F. Schatz, R. Stehle, H.-M. Uhde, *J. Vac. Sci. Technol. A* **1999**, *17*, 2318. b) D. G. de Oteyza, E. Barrena, J. O. Osso, H. Dosch, S. Meyer, J. Pflaum, *Appl. Phys. Lett.* **2005**, *87*, 183504-1-3.

[12] Y. Wakayama, *J. Phys. Chem. C* **2007**, *111*, 2675.

[13] D. G. de Oteyza, E. Barrena, H. Dosch, Y. Wakayama, *Phys. Chem. Chem. Phys.* **2009**, DOI:10.1039/B903116B.

[14] E. Barrena, D. G. de Oteyza, H. Dosch, Y. Wakayama, *ChemPhysChem.* **2007**, *8*, 1915.

[15] A. Gerlach, F. Schreiber, S. Sellner, H. Dosch, I. A. Vartanyants, B. C. C. Cowie, T.-L. Lee, J. Zegenhagen, *Phys. Rev. B* **2005**, *71*, 205425-1-7.

[16] While the quantitative values of charge transfer based on the Mulliken population analysis should be taken with care, the trend and relative changes are considered reliable. a) R. S. Mulliken, *J. Chem. Phys.* **1955**, *23*, 1833. b) C. Fonseca Guerra, J.-W. Handgraaf, E. J. Baerends, F. M. Bickelhaupt, *J. Comp. Chem.* **2004**, *25*, 189.

[17] J. Stöhr, *NEXAFS Spectroscopy*, Springer Series in Surface Sciences, Springer, Heidelberg, Germany **2003**.

[18] K. Takeuchi, A. Suda, S. Ushioda, *Surf. Sci.* **2001**, *489*, 100.

[19] G. Witte, S. Lukas, P. S. Bagus, C. Wöll, *Appl. Phys. Lett.* **2005**, *87*, 263502-1-3.

[20] The absence of resonances in additionally performed resonant photoemission measurements on single component and binary layers indicates a fast charge transfer between molecules and substrate, which is plausibly also related to the strong electronic molecule-substrate coupling. L. Wang, W. Chen, A. T. S. Wee, *Surf. Sci. Rep.* **2008**, *63*, 465.

[21] J. A. Knapp, F. J. Himpsel, D. E. Eastman, *Phys. Rev. B* **1979**, *19*, 4952.

[22] S. G. Louie, P. Thiry, R. Pinchaux, Y. Pétroff, D. Chandesris, J. Lecante, *Phys. Rev. Lett.* **1980**, *44*, 549.

[23] The particular sensitivity of the −3.55 eV bulk state to interacting adsorbates, in contrast to the minor changes observed in the −2.72 eV peak, is understood in the light of their distinct atomic wave function nature. Assuming, as usual for angle-resolved photoemission experiments, a vertical transition scheme within the reduced bulk Brillouin zone of Cu, the 130 eV photon energy excitation is equivalent to that of 26 eV [21,22], thats is, both allow us to probe Cu bulk states right at the Γ point. Therefore, the main peak at −3.55 eV in the clean Cu(111) spectrum belongs to the $\Gamma_{25'}$ symmetry point, namely pure $d_{3z^2-r^2}$-like atomic wave functions that extend perpendicular to the surface plane, whereas the −2.72 eV peak corresponds to the Γ_{12} symmetry point with $d_{xz,yz}$-like wave functions whose probability density is equally distributed both in and out of the surface plane.[21] As a consequence, the −3.55 eV $d_{3z^2-r^2}$-like state is more likely to interact and hybridize with adsorbate electronic states of similar energy. An Umklapp effect as the origin for this spectral change can be discarded due to the large energy shift from −3.55 to −4.3 eV, in combination with the relatively low dispersion of this electronic state [21] and the large unit cell dimensions of the crystalline overlayer.

[24] According to the theoretical results one would expect changes in the widths of the DIP and F_{16}CuPc resonances. However, because the various fitted resonances typically correspond to a superposition of manifold transitions combining the various initial and final states [5,17,25] such an observation is hampered.

[25] M. Alagia, C. Baldacchini, M. G. Betti, F. Bussolotti, V. Carravetta, U. Ekström, C. Mariani, S. Stranges, *J. Chem. Phys.* **2005**, *122*, 124305-1-6.

[26] The calculations are first performed for gas phase molecules. Then we calculate the effect of charge removal on the core-level binding energies. Finally, the influence of the substrate is mimicked calculating the core-level energies upon charge transfers as obtained from the Mulliken population analysis. This approach shows limited reliability and is expected to account for the difference between experiment and theory. However, the relative energy difference between the different components of the atomic species are reasonably well reproduced.

[27] I. Horcas, R. Fernández, J. M. Gómez-Rodríguez, J. Colchero, J. Gómez-Herrero, A. M. Baro, *Rev. Sci. Instrum.* **2007**, *78*, 013705-1-8.

[28] D. G. de Oteyza, E. Barrena, Y. Zhang, T. N. Krauss, A. Turak, A. Vorobiev, H. Dosch, *J. Phys. Chem. C* **2009**, *113*, 4234.

[29] L. Floreano, A. Cossaro, R. Gotter, A. Verdini, G. Bavdek, F. Evangelista, A. Ruocco, A. Morgante, D. Cvetko, *J. Phys. Chem. C* **2008**, *112*, 10794.

[30] L. Floreano, G. Naletto, D. Gvetko, R. Gotter, M. Malvezzi, L. Marassi, A. Morgante, A. Santaniello, A. Verdini, F. Tommasini, G. Tondello, *Rev. Sci. Instrum.* **1999**, *70*, 3855.

[31] G. T. Velde, F. M. Bickelhaupt, E. J. Baerends, C. F. Guerra, S. J. A. Van Gisbergen, J. G. Snijders, T. Ziegler, *J. Comput. Chem.* **2001**, *22*, 931.

[32] S. H. Vosko, L. Wilk, M. Nusair, *Can. J. Phys.* **1980**, *58*, 1200.

[33] J. M. Soler, E. Artacho, J. D. Gale, A. Garcia, J. Junquera, P. Ordejón, D. Sánchez-Portal, *J. Phys. Cond. Matter* **2002**, *14*, 2745.

[34] J. P. Perdew, Y. Wang, *Phys. Rev. B* **1992**, *45*, 13244.

[35] M. Fuchs, M. Scheffler, *Comput. Phys. Commun.* **1999**, *119*, 67.

[36] N. Atodiresei, V. Caciuc, P. Lazic, S. Blügel, *Phys. Rev. Lett.* **2009**, *102*, 136809-1-4.